

BUREAU INTERNATIONAL DES POIDS ET MESURES



Anelasticity of Cu-Be at very low strain frequencies
preliminary measurements

by T.J. Quinn and C.C. Speake

PAVILLON DE BRETEUIL
F-92312 SÈVRES CEDEX

Anelasticity of Cu-Be at very low strain frequencies
preliminary measurements

by T.J. Quinn and C.C. Speake

Abstract

This note reports the preliminary results of a study of the anelasticity of a Cu - 1,8 % Be alloy at strain frequencies between 10^{-2} and 10^{-3} Hz. The measurements were made using a vertical dumb-bell pendulum suspended near its centre of mass by a flexure pivot made from the Cu-Be alloy under test. Unexpectedly large anelastic effects were found at the lowest frequencies. A mechanism explaining the observed behaviour is proposed based upon a hierarchical relaxation process having a continuum of relaxation times. Further measurements are underway.

1. INTRODUCTION

The presence of small anomalies in the behaviour of the BIPM flexure-strip balance⁽¹⁾ led us to think that the flexure might be showing signs of anelasticity. The complexity of the balance, however, made it difficult to carry out a study of the anelastic behaviour of the flexure pivot alone. A sabbatical year at the Cavendish Laboratory, Cambridge, gave one of us (TJQ) the opportunity of building an apparatus that was specifically designed to study anelasticity. This was a vertical dumb-bell pendulum suspended near its centre of mass by a Cu-Be flexure pivot of the type developed for the BIPM flexure-strip balance. The anomalies observed in the behaviour of the balance appeared to be

consistent with the presence of a small anelastic after effect following an angular displacement of the beam of about 6×10^{-5} radians. The recovery time of the effect appeared to be about five minutes. The aim of the experiments at Cambridge was, therefore, to look for and if possible measure, the anelastic behaviour of a Cu-Be flexure under similar conditions of tensile stress and in a similar frequency range to those observed at BIPM.

The flexure strips in question were made from a precipitation-hardened Cu - 1,8 % Be alloy made by Telcon Metals Ltd. under the trade name Be 250. The strips were 50 μm thick, 2 mm long and 20 mm wide and were made from a solid block of alloy as shown in Fig. 1 and described in reference (1). When used in the balance the strip supports a mass of about 4 kg which leads to a stress in the strip of about 5% of the yield stress.

We were unable to find reports of any previous work in which the anelasticity of Cu-Be had been examined under conditions remotely resembling those of interest here. Practically all previous studies of the anelasticity of similar Cu-Be alloys had been carried out at much higher frequencies and after strain cycles of much larger amplitude.

2. THE PENDULUM

The pendulum is shown in Fig. 2. It consists of two thin walled aluminium alloy (duralumin) tubes (A & B) supporting at their extremities 1,2 kg phosphor-bronze balls (C & D) and joined at the centre to a duralumin piece (E) designed to rest upon the flexure pivot. The flexure pivot in turn rests on a duralumin block (F) as shown in Fig. 3. Fig. 4 shows the pendulum in place resting on the flexure pivot.

The upper phosphor-bronze ball is enclosed in a cap (G) in Fig. 5 that carries a pair of flat plates (H), used in the capacitance

position sensor and for electrostatic servo control. Concentric with the pendulum is a rigid duralumin cylinder (J) which carries two pairs of fixed electrodes (K) and (L) for the position sensor and servo-control.

The whole of the pendulum is enclosed in a stainless steel vacuum chamber (Fig. 6). Preliminary pumping is by means of a rotary pump and then a sorption pump. During operation the pressure is maintained below about 10^{-4} Pa by an ion pump.

Adjustment of the period of the pendulum can be made from outside the vacuum chamber through the rotary lead-through (M in Fig. 6). This can engage a nut on a screw protruding from the lower end of the pendulum and so raise or lower the centre of mass of the pendulum by a small amount. In this way the period could be adjusted in the range from 125 s to 690 s.

The centre base plate upon which the pendulum was mounted served as the main supporting plate for the vacuum chamber. It was also connected to a platform resting on a steel frame attached to concrete blocks on the floor of the laboratory. The platform could be adjusted in level by the three micrometer screws upon which it rested. On the top of the vacuum chamber a microscope was mounted by means of which the amplitude of free oscillation of the pendulum could be observed through a glass window which formed the top of the vacuum chamber. Below the vacuum chamber a 14 kg phosphor-bronze ball was mounted on a rotatable platform. This was used for calibration of the servo-system by providing a known gravitational attractive force to the pendulum.

3. THE SERVO-CONTROL

The position of the top of the pendulum with respect to the fixed cylinder (Fig. 5) was measured using a capacitance transducer. Servo

control was carried out by means of electrostatic forces applied to the plates fixed to the pendulum. The servo control was designed to provide proportional differential and integral control and incorporated various features required for the two different types of measurement described below. The pre-amplifier was mounted as close as possible to the pendulum and was attached near the top of the vacuum chamber.

4. THE MEASUREMENTS

The whole mechanical and electronic system was designed with two types of measurement in view. The first was a measurement of the decay of the amplitude of free oscillation and the second was the measurement of the anelastic after effect following angular offset of the pendulum.

4.1.- Elementary theory of the decay of free oscillations

Let us assume the the equation of motion of the pendulum is given by

$$I \ddot{\theta} + (c - mgh)\theta = 0 \quad (1)$$

where I is the moment of inertia about the axis of rotation, c the flexure stiffness of the suspension, m the mass of the pendulum and h the distance of its centre of mass above the centre of rotation. The stiffness of the flexure is given by ⁽¹⁾

$$c = (WEH)^{\frac{1}{2}} \operatorname{cosech} \alpha l \quad (2)$$

where $W = mg$, E is Young's modulus, H is the second moment of area of the flexure cross section, $\alpha = (W/EH)^{\frac{1}{2}}$ and l the length of the flexure.

In the presence of anelasticity we can write

$$E = E_0 + i\Delta \quad (3)$$

and thus

$$c = (WE_0H)^{\frac{1}{2}} \left(1 + \frac{i\Delta}{2E}\right) \quad (4)$$

$$= c_0 \left(1 + \frac{i\Delta}{2E}\right) \quad (5)$$

Equation (1) becomes

$$I \ddot{\theta} + (c_0 - mgh)\theta + i\delta\dot{\theta} = 0 \quad (6)$$

where $\delta = \frac{c_0 \Delta}{2E}$.

$$\text{Let } \theta = e^{(i\omega - \gamma)t} \quad (7)$$

Thus

$$(i\omega - \gamma)^2 + \frac{i\delta}{I} + \frac{c_0 - mgh}{I} = 0 \quad (8)$$

from which we can deduce that

$$\gamma = \frac{\delta}{2I\omega} \quad (9)$$

We define the loss coefficient η by

$$\eta = \frac{1}{\pi} \log \left(\frac{A_n}{A_{n+1}} \right) \quad (10)$$

where A_n and A_{n+1} are the amplitudes of successive oscillations of the pendulum. We can, therefore, deduce that

$$\eta = \frac{1}{\pi} \log \left[\frac{e^{-\gamma t}}{e^{-\gamma(t+T)}} \right] = \frac{\gamma T}{\pi} \quad (11)$$

or
$$\eta = \frac{\delta}{I\omega^2} \quad (12)$$

Measurements of η as a function of frequency ω can thus give information on δ . As we shall see, it was observed that η increased as $1/\omega^2$ implying that δ was independent of frequency. However, according to the theory of a generalized susceptibility δ must be a function of frequency. This is discussed in Section 5.

4.2.- Experimental results

The results of the measurements of η are shown in Fig. 7. These were obtained from measurements of the decay of free oscillations in the frequency range from 5×10^{-2} to 9×10^{-3} rad s⁻¹ (periods from 125 s to 690 s). The amplitudes of oscillation of the pendulum were of the order of 1 mrad and no amplitude dependency of η was observed. Since, however, the measurements of amplitude were made visually and were very tedious, no systematic investigation of amplitude dependency was made.

In order to check that the mechanism which led to the observed ω^{-2} dependency of η was a bulk property of the flexure material and not a surface property due to surface damage on grinding, a layer 5 μm thick was electrolytically removed from the surface and a second set of measurements made. There are also shown in Fig. 7 and it is clear that they do not differ significantly from the first set.

The depth of surface damage was estimated to be of the order of 5 μm from measurements of micro hardness made on Cu-Be strips manufactured in the same way as the flexures. A significant increase in hardness was found that did not extend below a depth of about 5 μm .

We conclude, therefore, that what we observed was a bulk property of the alloy.

4.3.- The anelastic after effect, results of experiments

In the presence of anelasticity a stress introduced into the flexure by applying an offset to the pendulum does not immediately disappear on removal of the offset. Instead, a residual stress, ΔE , is observed that dies away with a characteristic decay time. This is illustrated in Fig. 8. ΔE is known as the anelastic after effect, which, in the case of the standard-linear solid is given by

$$\Delta E = A(1 - e^{-T/T_0}) e^{-t/T_0} \quad (13)$$

where A is the magnitude of the offset, T the time for which it is maintained and T_0 is the time constant of the decay of ΔE . The anomalies observed in the behaviour of the flexure-strip balance were considered to be due to the presence of such an anelastic after effect.

The experiments made with the pendulum consisted of the application of angular offsets to the pendulum of about one milli-radian for periods of between one minute and two hours and the observation of the return to equilibrium of the servo voltage after abrupt removal of the offset. The servo control was such that on removal of the offset the pendulum returned to its original position to within about 10^{-8} rad after only a few seconds.

The magnitude of the anelastic after effect was established by calibration of the system using the gravitational attraction of a 14 kg phosphor-bronze sphere. The sphere was placed on a rotating table close to the lower ball of the pendulum. On rotating the table so that the sphere moved from one side of the pendulum to the other a change in torque of $4,5 \times 10^{-8}$ Nm took place.

Two series of measurements of ΔE as a function of T were made, one with an offset of $1,5 \times 10^{-3}$ rad and one with an offset nearly twice as

large, $2,9 \times 10^{-3}$ rad. As expected, the magnitude of ΔE appeared to increase linearly with the size of the offset. Fig. 8 shows the results of all the measurements that were made. The results were first of all fitted to an equation of the form given in (13) with $A = \theta \cdot [1,1 \times 10^{-4} \text{ Nm rad}^{-1}]$ where θ is the angle of offset and T_0 , the time constant, equal to about 18 minutes.

Examination of the chart recordings, however, led to the conclusion that a simple exponential decay of the anelastic after effect was probably not what was observed. The short term decay lasting about 5 minutes appeared to follow an exponential curve, but this was followed by a much slower decay that lasted at least 30 minutes.

We suggest that this behaviour might be due to the particular conditions of the experiment, namely, that the very small changes in strain, resulting from the offsets, take place in the presence of the much larger continuous strain resulting from the weight of the pendulum. In the presence of this continuous stress it may be that the decay of the anelastic after effect takes place in a hierarchical regime in which successive levels of dislocation unlocking occur. Were this to be the case the simple exponential decay predicted by equation (13) would no longer be observed.

5. AN ANELASTIC SOLID HAVING A CONTINUUM OF RELAXATION TIMES

5.1.- Mathematical model

A material which has a single relaxation process can be represented by the Maxwell model shown in figure 9a and it can easily be shown that the following relationship exists between an applied stress, σ , and the resulting strain, ϵ ,

$$\epsilon E + \dot{\epsilon} \tau (E + \delta E) = \sigma + \dot{\sigma} \tau \quad (14)$$

where E is the relaxed modulus, δE is the modulus defect and the relaxation time constant, τ , is given as the ratio of the dashpot viscosity and δE . For what follows it will be convenient to express equation 14 in terms of Laplace transforms with the Laplace variable s ,

$$\frac{\sigma(s)}{\varepsilon(s)} = E + \delta E \frac{s\tau}{1 + s\tau}. \quad (15)$$

Unfortunately, as was seen in Section 3, such a simple model is inadequate for describing the behaviour of the beryllium-copper flexures. Instead, we shall consider the model illustrated in figure 9b where an infinite number of spring-dashpot combinations have been added having a continuum of relaxation time constants, up to a maximum (τ_∞) and each having an equal relaxation amplitude ($\delta E/\tau_\infty$). Equation 15 can now be expressed in terms of an integral

$$\frac{\sigma(s)}{\varepsilon(s)} = E + \int_0^{\tau_\infty} \frac{\delta E s\tau}{1 + s\tau} \frac{d\tau}{\tau_\infty}. \quad (16)$$

Using the above expression with the appropriate Laplace variable we can calculate the modulus relaxation in response to sinusoidal excitation (free oscillation of the pendulum) or static changes in angular deflection of the flexure. In either case we can substitute the appropriate form of the modulus calculated using equation 16 into the usual expression for the flexure restoring torque, equation 2.

$$c_0 = (WEH)^{\frac{1}{2}} \operatorname{cosech}(\alpha l) \quad (17)$$

In the approximation that the anelastic component of the modulus (the second term in equation 16) is much smaller than E and that $\alpha l \gg 1$, we can write

$$c_0' = c_0 \left(1 + \frac{\delta E}{2E\tau_\infty} \int_0^{\tau_\infty} \frac{s\tau}{1 + s\tau} d\tau \right). \quad (18)$$

5.2. The anelastic after effect

If the flexure is subject to a step deflection $\theta(t)$ as follows

$$\theta(t) = 0 \quad t < -T \quad (19a)$$

$$\theta(t) = \theta_0 \quad -T < t < 0 \quad (19b)$$

$$\theta(t) = 0 \quad 0 < t \quad (19c)$$

which implies

$$\theta(s) = \frac{\theta_0}{s} e^{sT} \quad -T < t < 0 \quad (19d)$$

$$\theta(s) = \frac{\theta_0}{s} (e^{sT} - 1) \quad 0 < t, \quad (19e)$$

then we can calculate the torque required to maintain zero deflection as

$$c(t) = c_0 \theta_0 + c_0 \theta_0 \frac{\delta E}{2E} \cdot \frac{1}{\tau_\infty} \int_0^{\tau_\infty} e^{-(t+T)/\tau} d\tau$$

for $-T < t < 0$ (20a)

$$\text{and } c(t) = -c_0 \theta_0 \frac{\delta E}{2E} \frac{1}{\tau_\infty} \left\{ 1 - \int_0^{\tau_\infty} e^{-T/\tau} d\tau \right\} \int_0^{\tau_\infty} e^{-t/\tau} d\tau$$

for $0 < t$ (20b)

It can be shown that the integrals can be calculated as

$$\int_0^{\tau_\infty} e^{-t/\tau} d\tau = \left\{ \tau_\infty e^{-t/\tau_\infty} + t \text{Ei}(-t/\tau_\infty) \right\} \quad (21)$$

where $\text{Ei}(-t/\tau_\infty)$ is the exponential integral function.

5.3.- The dynamic damping due to anelasticity

The differential equation describing the free oscillation of the pendulum, equation (1), can be written as

$$I\ddot{\theta} + (Wh + c_0(s))\theta = 0 \quad (22)$$

If we again suppose a solution for free oscillation

$$\theta = \theta_0 e^{st} \text{ with } s = i\omega - \gamma \quad (23)$$

where ω is the angular frequency of free oscillations and γ^{-1} is the characteristic time of the decay of oscillation amplitude, then, on substitution of equation 23 into equation 22, we obtain the characteristic equation,

$$s^2 I + (Wh + c_0^{\cdot}(s)) = 0 \quad (24)$$

After evaluating the integral in equation 16 this becomes

$$I(i\omega - \gamma)^2 + Wh + c_0 + c_0 \frac{\delta E}{2E} \cdot \frac{1}{\tau_{\infty}} \left\{ \tau_{\infty} - \frac{\ln(1 + (i\omega - \gamma) \tau_{\infty})}{(i\omega - \gamma)} \right\} = 0. \quad (25)$$

Taking the imaginary part of this equation we can numerically solve for $\gamma(\omega)$ and then calculate the logarithmic decrement

$$\eta = \frac{2\gamma}{\omega}. \quad (26)$$

5.4.- Comparison of theory with experiment

Figure 10 shows an experimental curve of the type given in equation 20b with values of τ_{∞} and $\frac{c_0 \delta E}{2E}$ chosen to give the best fit to one of the experimentally observed curves (P of Fig. 8). The values $\tau_{\infty} = 2,2 \times 10^3$ s and $\frac{c_0 \delta E}{2E} = 1 \times 10^{-4}$ Nm rad⁻¹ result in an extremely good fit to the data.

Figure 7 shows the theoretical and experimental results of the dynamic damping measurements and here there does seem to be some discrepancy. The theoretical curve was calculated using the same values of τ_{∞} and $c_0\delta E/2E$ as for Fig. 10.

6. CONCLUSIONS

The observed anelastic behaviour of the Cu-Be flexure cannot be explained on the basis of a single relaxation process. A more complex mechanism for the anelastic behaviour based upon a hierarchical structure of dislocation locking mechanisms having a continuum of relaxation time leads to a much better fit to the data. Some experiments made using an aluminium alloy flexure and also an agate knife edge indicated similar ω^{-2} dependency of damping upon frequency. This suggests that the mechanism responsible for damping in Cu-Be may not be unique to this alloy. Further experiments on Cu-Be are underway with a view to obtaining more accurate data so that the theoretical model can be more rigorously tested. Finally we note that a damping-frequency characteristic of the type observed leads directly to $1/f$ noise at frequencies above $1/\tau_{\infty}$ and it may will be possible to measure experimentally the intrinsic noise of the Cu-Be flexures.

Acknowledgements

The authors are pleased to acknowledge the contribution made to this work by Mr. Ray Flaxman who constructed the apparatus with which the measurements were made, Mr. Norman Bett who designed and built the electronic control systems and Dr. M.H. Brown for useful discussions, all of whom are at the Cavendish Laboratory. One of us (TJQ) is

Captions to figures

- Fig. 1 The flexure pivot is machined to the form shown in 'a' while the Cu-Be alloy is in the solution heat-treated state. After precipitation hardening the flexure is ground to the dimensions and shape shown in 'b'
- Fig. 2 The pendulum: A and B are thin-walled aluminium-alloy tubes, C and D are 1,2 kg phosphor-bronze balls (D is inside B) and E is an aluminium-alloy piece designed to rest upon the flexure pivot shown in Fig. 1.
- Fig. 3 The flexure pivot F resting on its support S ready to be pushed into position to take the pendulum.
- Fig. 4 The pendulum in place resting on the flexure pivot.
- Fig. 5 The top of the completed assembly: G, a cap (covering the upper phosphor-bronze ball C) carrying a pair of flat plates H used in the capacitance position-sensor and servo-control system. J a rigid duralumin tube supporting the fixed pairs of capacitance plates K and L.
- Fig. 6 The stainless steel vacuum chamber enclosing the pendulum.
- Fig. 7 Loss coefficient η as a function of frequency for Cu-Be flexure strip:
- experimental results, first series of measurements
 - experimental results, second series of measurements made after 5 μm thick surface layers of Cu-Be removed by electropolishing.
 - linear fit to experimental data showing $\eta \propto 1/\omega^2$
 - theoretical curve calculated from equations 25 and 26

grateful to the Master and Fellows of Christ's College Cambridge for the award of a Visiting Fellowship, to the Royal Society for a Visiting Fellowship, to the Cavendish Laboratory, in particular Dr. A.J.F. Metherell, for research facilities and to the CIPM for having granted permission for him to spend a year in Cambridge.

Reference

1. QUINN, T.J., SPEAKE C.C. and DAVIS R.S., A 1 kg Mass comparator Using Flexure-Strip Suspensions: Preliminary Results. Metrologia, 23, 1986/87, pp. 87-100.

Fig. 8 The anelastic after effect, ΔE , as a function of time of offset, T , and magnitude of offset, A , observed for the Cu-Be flexure strip. The data from point P is used in Fig. 10.

Fig. 9 (a) The simple Maxwell model of an anelastic solid having a single relaxation process

(b) An anelastic solid having an infinite number of relaxation processes having a continuum of time constants up to a maximum of τ_{∞} and each having the same relaxation amplitude $\delta E/\tau_{\infty}$.

Fig. 10 The anelastic after effect ΔE :
+++ data points from an experimentally observed curve (P of Fig. 8) for the Cu-Be flexure strip
— theoretical curve for the solid of Fig. 9b calculated from equation (20b) with $\tau_{\infty} = 2200$ s and $c_0 \delta E/2E = 10^{-4}$ Nm rad $^{-1}$.

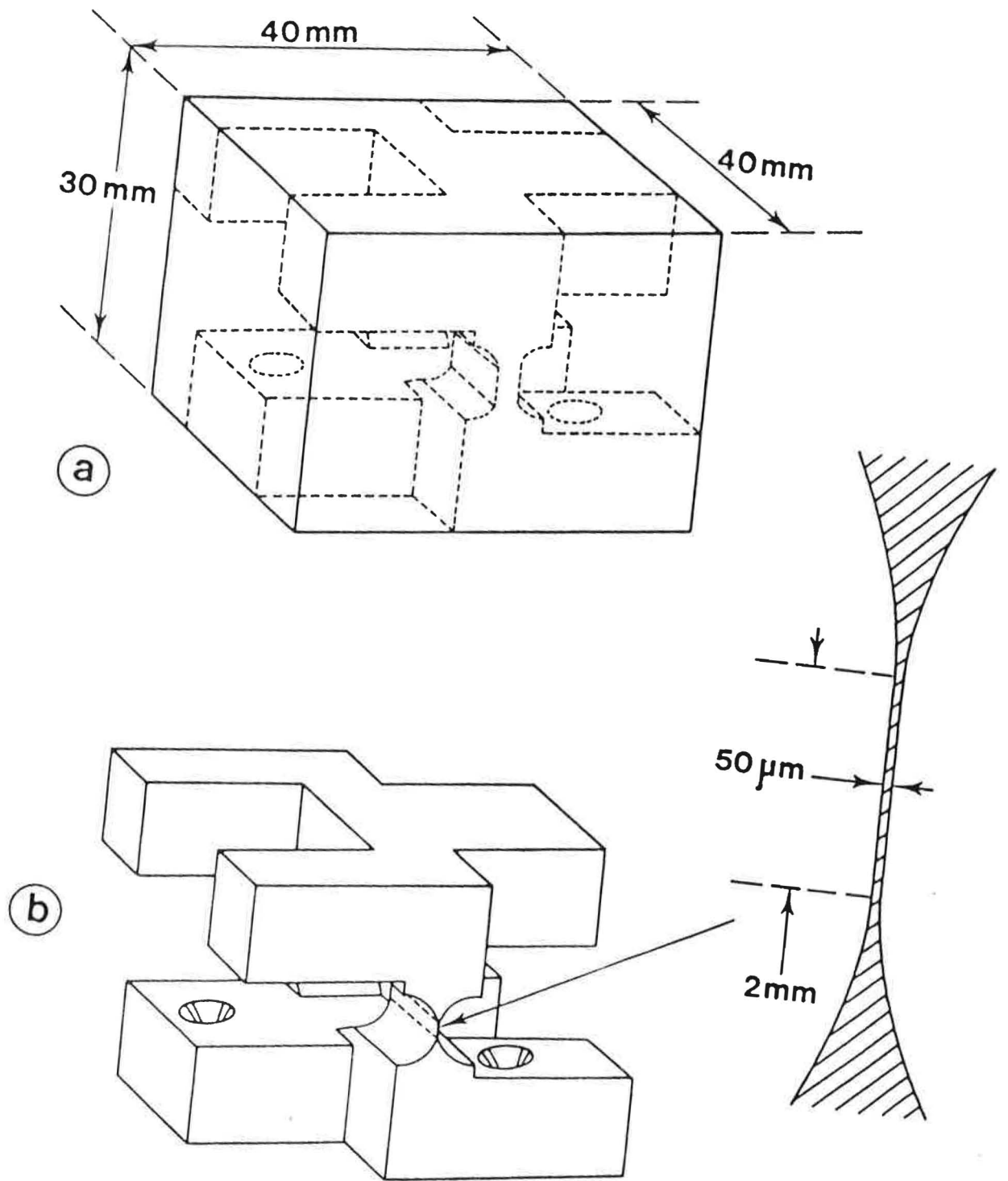


Fig. 1

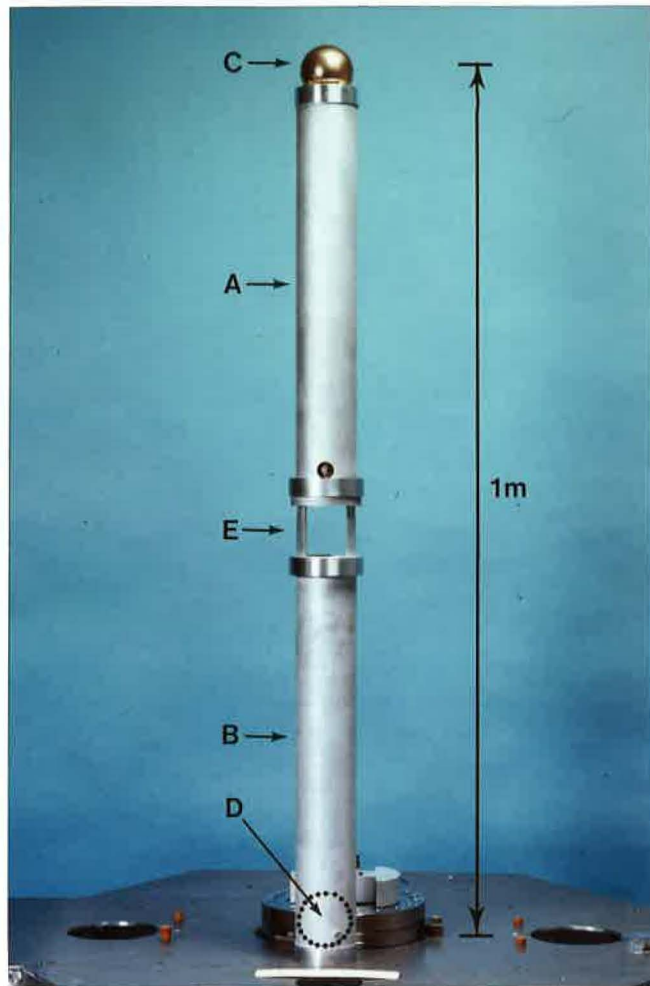


Fig. 2

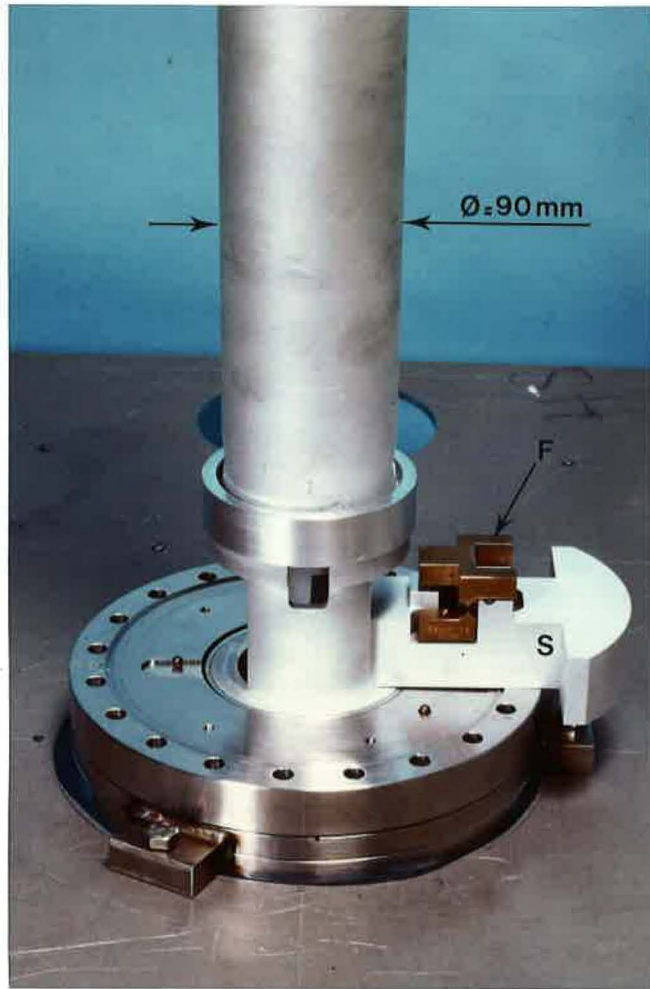


Fig. 3

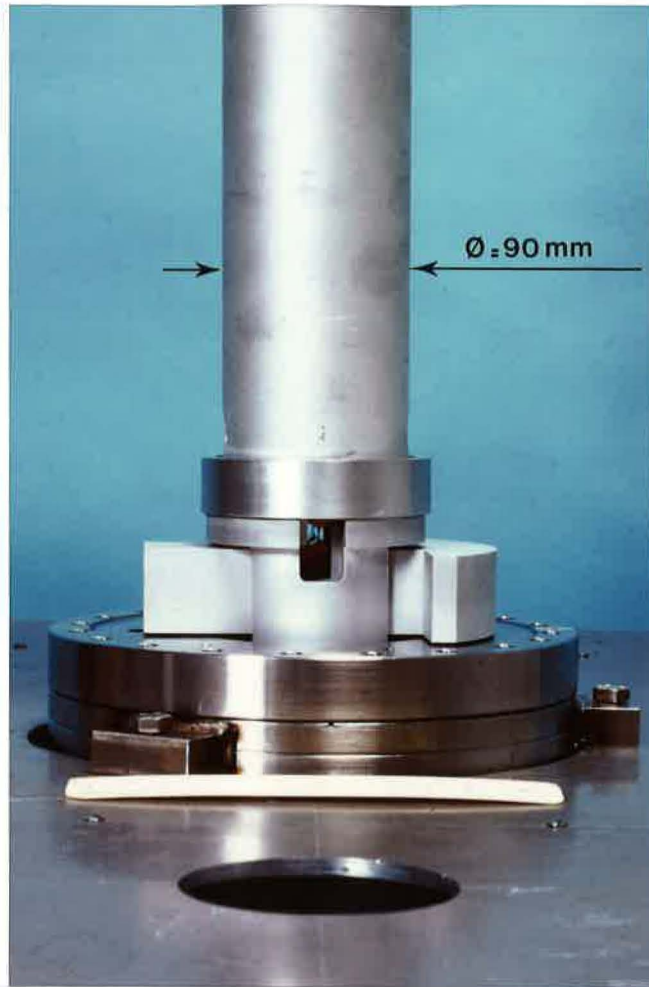


Fig. 4

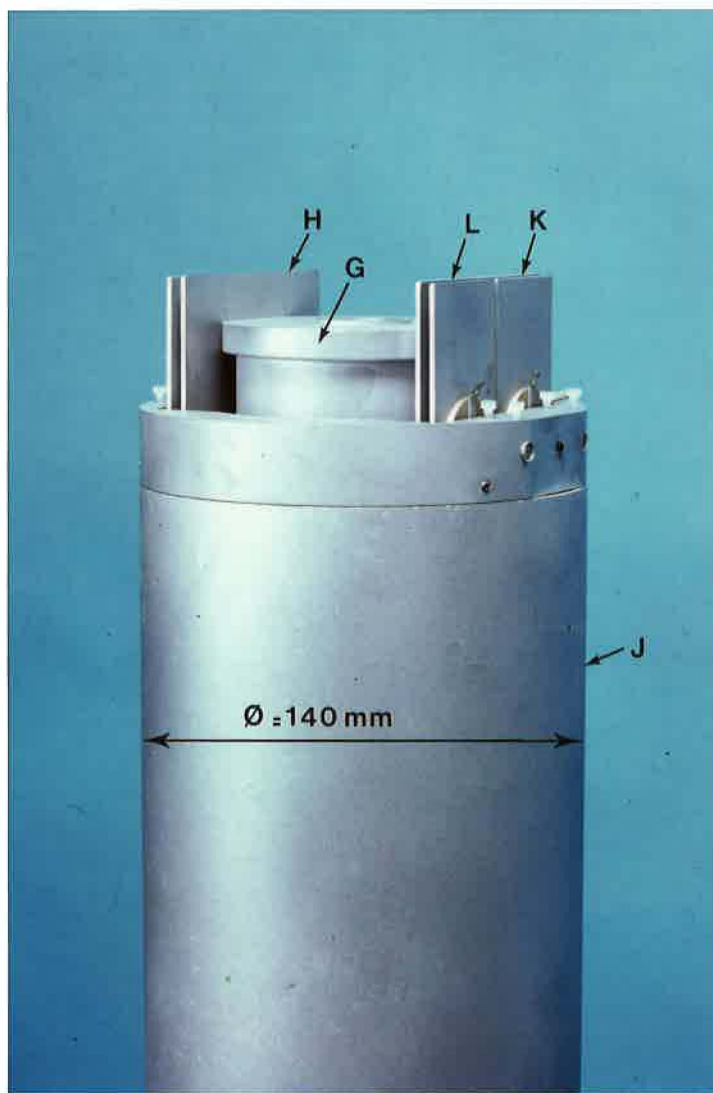


Fig. 5

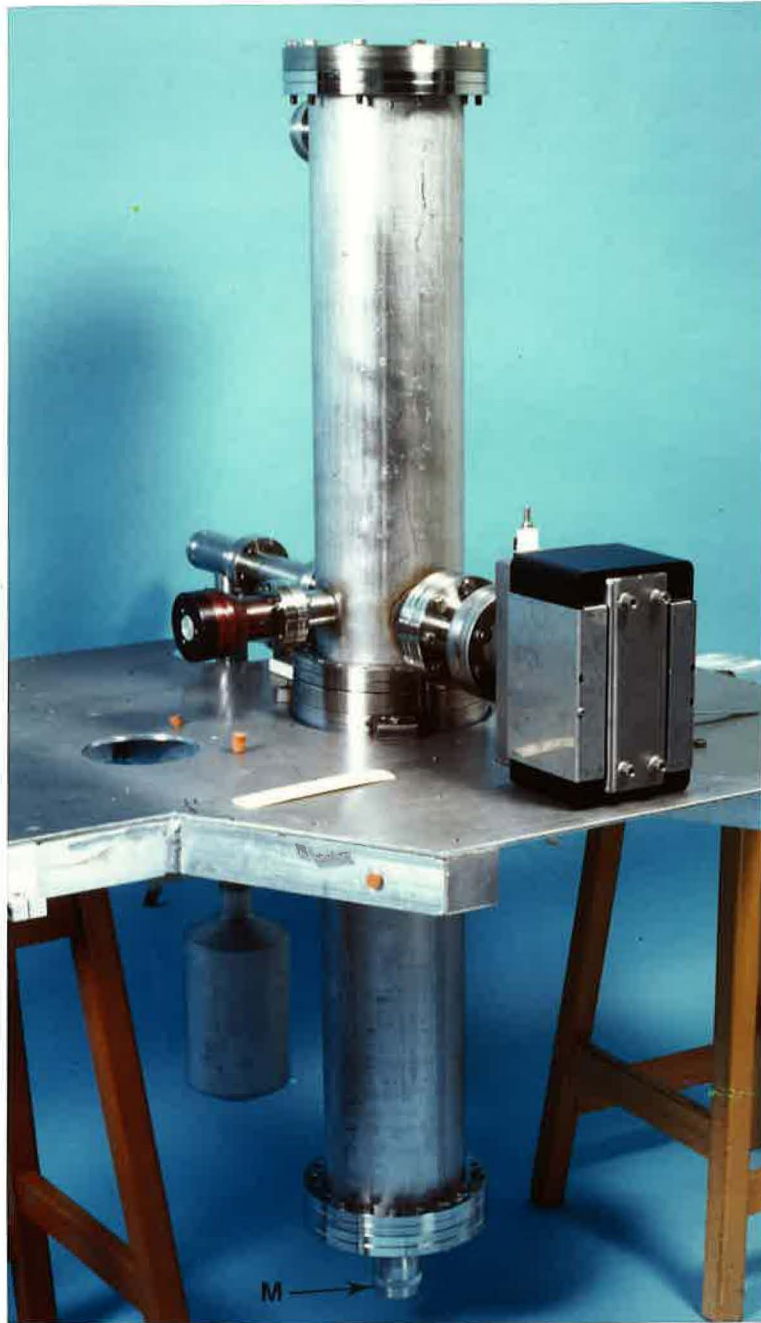


Fig. 6

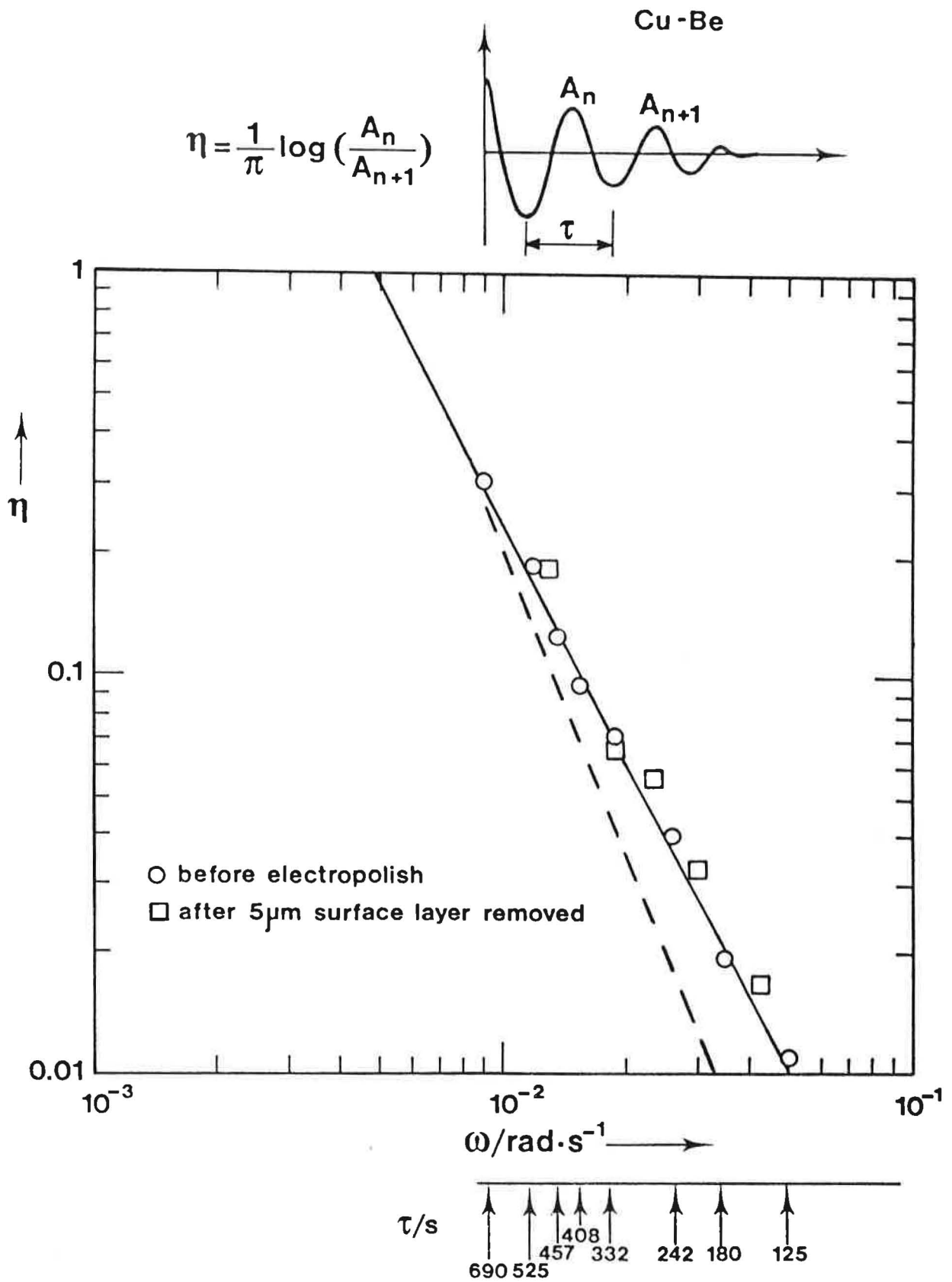


Fig. 7

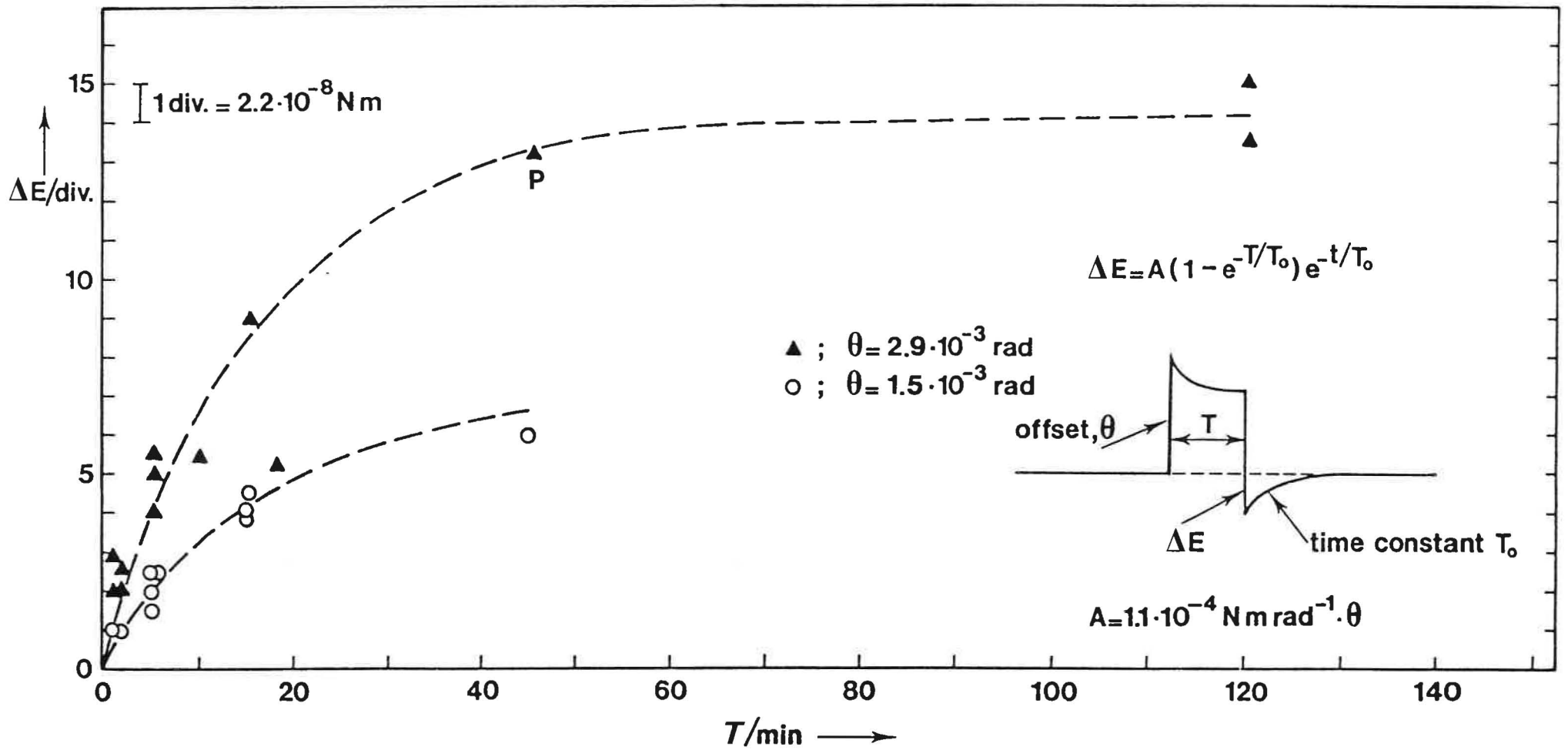


Fig. 8

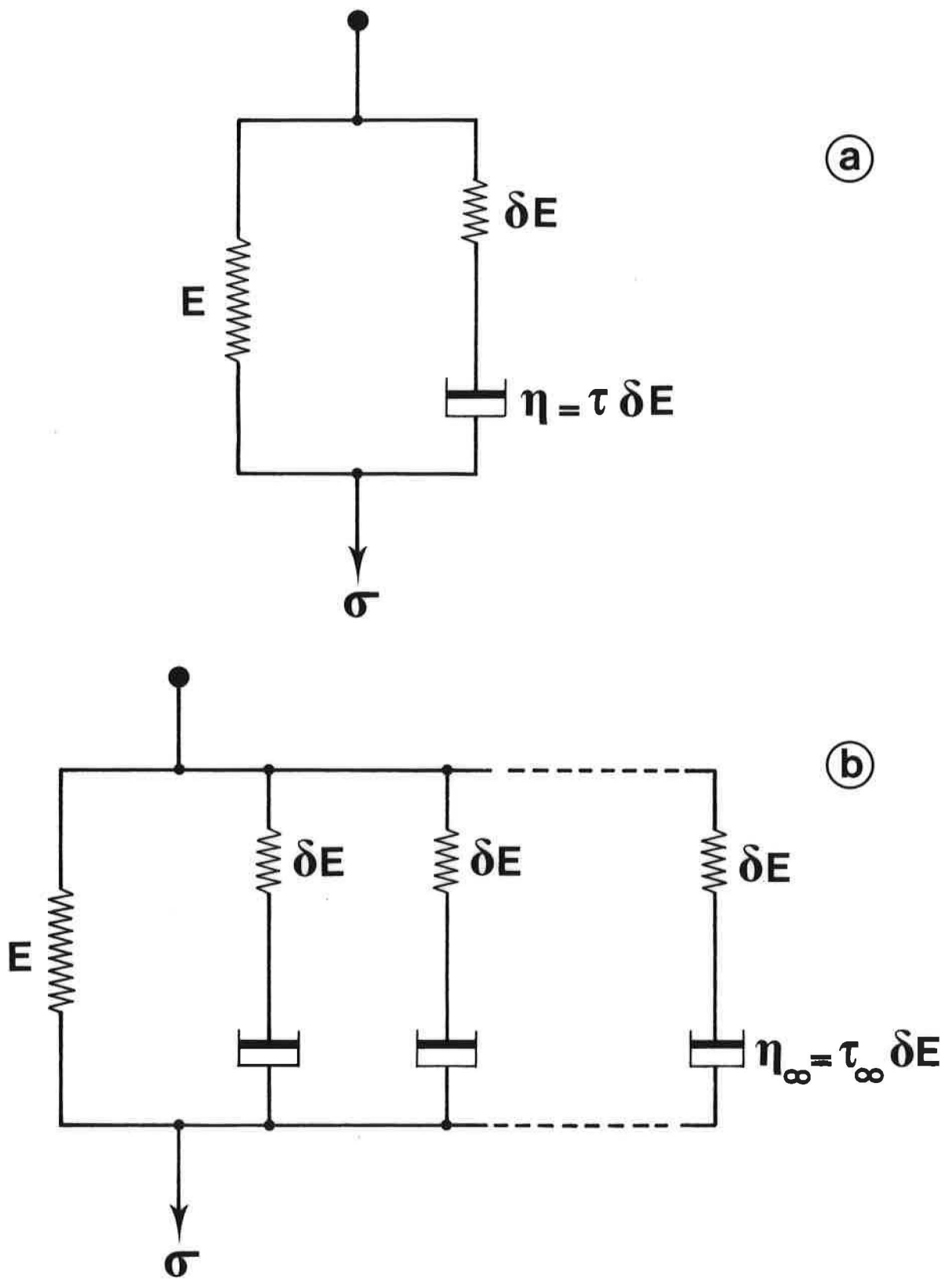


Fig. 9

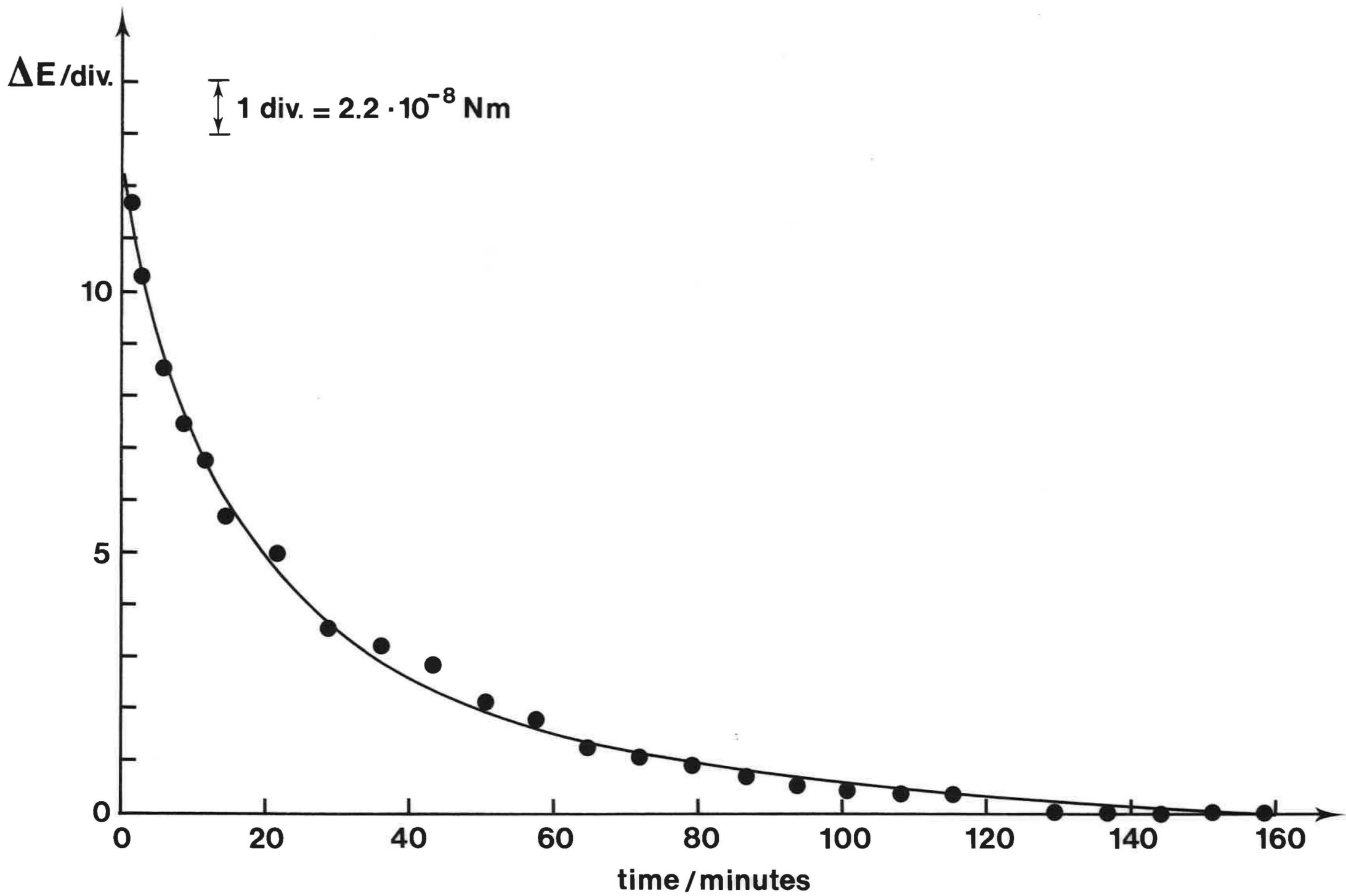


Fig. 10